International Journal of Applied Pharmaceutics

ISSN- 0975-7058 Vol 16, Issue 3, 2024

Original Article

STUDY OF THE INHIBITORY EFFECTS OF VITAMIN E DERIVATIVES ON MITOCHONDRIAL COMPLEX II SUBUNIT USING MOLECULAR DOCKING

IRMA RATNA KARTIKA[1,2*], TENI ERNAWATI[3], WIDIA A. JUSMAN[4], MOHAMAD SADIKIN[4]

[1]Doctoral Program of Biomedical Science, Faculty of Medicine, Universitas Indonesia, Jakarta, Indonesia. [2]Program Study of Chemistry, Faculty of Mathematics and Natural Sciences, Universitas Negeri Jakarta, Jakarta, Indonesia. [3]Research Center for Medicinal Raw Materials and Traditional Medicine, National Research and Innovation Agency-BRIN Puspiptek Serpong, Banten, Indonesia. [4]Department of Biochemistry and Molecular Biology, Faculty of Medicine, Universitas Indonesia, Jakarta, Indonesia

[*]Corresponding author: Irma Ratna Kartika; [*]Email: irmaratna@unj.ac.id

Received: 03 Dec 2023, Revised and Accepted: 12 Feb 2024

ABSTRACT

Objective: The goal of this study was to create vitamin E derivatives and explore their potential anticancer properties using a computational approach.

Methods: The Steglich method was used for the synthesis of the vitamin E-fatty acid (pentanoic acid, heptanoic acid, and octanoic acid) derivatives, with *N,N'*-dicyclohexylcarbodiimide (DCC) and 4-dimethylaminopyridine (DMAP) as the catalysts. The structure of the synthesized products was determined by ultraviolet-visible (UV-Vis) spectroscopy, fourier transform infrared (FTIR) spectroscopy, and liquid chromatography-mass spectrometry (LC-MS). Molecular docking was carried out on the succinate dehydrogenase (SDH) enzyme using AutoDockTools.

Results: α–Tocopherol pentanoate (α–TP), α–tocopherol heptanoate (α–TH), and α–tocopherol octanoate (α–TO) were the three vitamin E derivatives synthesized in this study. Based on the results of molecular docking, the novel compounds (α–TP, α–TH, and α–TO) generated bond energies of-10.57,-9.61, and-9.20 kcal/mol, respectively.

Conclusion: All newly synthesized compounds exhibited lower binding affinity values than α–tocopherol (α–T). This confirms that these compounds might not provide greater advantages than α-tocopherol in terms of inhibitory effects on mitochondrial complex II (CII).

Keywords: Vitamin E, Pentanoic acid, Heptanoic acid, octanoic Acid, SDH

DOI: https://dx.doi.org/10.22159/ijap.2024v16i3.50040 Journal homepage: https://innovareacademics.in/journals/index.php/ijap

INTRODUCTION

Succinate dehydrogenase (SDH), also known as mitochondria complex II or succinate-ubiquinone oxidoreductase, is a mitochondrial enzyme that plays a role in both the citric acid cycle and the electron transport chain (ETC) across all living organisms [1]. This enzyme catalyzes the oxidation of succinate to fumarate and the reduction of ubiquinone (UbQ) to ubiquinol [2]. SDH comprises SDHA, SDHB, SDHC, SDHD, SDHAF1, SDHAF2 subunits [3], and exhibits tumor-suppressing effects [4]. A decreased SDH activity leads to the accumulation of succinate, thus triggering the stabilization of the hypoxia-inducible factor (HIF) through competitive inhibition of HIF prolyl hydroxylases [5]. A stabilized HIF triggers pseudo–hypoxia signaling, leading to angiogenesis, dysregulation of cell proliferation, and adhesion [6]. Accumulation of succinate is also linked to epigenomic changes that promote oncogenesis by inhibiting histone demethylation [7]. The decreased in SDH activity can arise from mutations in SDHA, SDHB, SDHC, SDHD, or SDHAF2 (SDHx genes) [8] and has been documented in gastrointestinal stromal tumor (GIST) [9], renal cell carcinoma (RCC) [10], pituitary adenoma (PA) [11], and pancreatic neuroendocrine tumor (PanNET) [12].

Foods and medicinal plants represent important resources for the discovery of novel and valuable therapeutic molecules [13]. Biomolecules exhibit remarkable diversity and possess potent antioxidant, anti-inflammatory, and anticancer properties [14]. Quantitatively, structure-activity relationship studies have indicated that biomolecules can serve as templates for chemical modifications to enhance the efficiency, safety, and bioavailability of compounds [13]. α–Tocopherol (α–T), a natural substance found in fats and oils from both animal and vegetable sources, is among these biomolecules [15]. Recent research has revealed the diverse biological functions of α–T, encompassing anti-inflammatory [16], anticancer, and antioxidant properties [17]. Extensive research on α–T has been conducted to modify its structure to generate vitamin E derivatives with antioxidant and anticancer properties [18]. The synthesis of α–tocopherol succinate (α–TS), a derivative of vitamin E, was accomplished through the combination of α–T and succinic acid [19]. In mouse models of breast cancer, α–TS substantially inhibited tumor progression [20]. This was achieved by α-TS blocking the UbQ binding sites of CII, leading to the generation of reactive oxygen species (ROS) and the subsequent induction of apoptosis [21]. α-TS acts dominantly downstream of any anti-apoptotic pro-survival activity resulting from erbB2 receptor tyrosine kinase signaling [22]. Meanwhile, α–tocopherol acetate (α–TA) was synthesized through the chemical acylation of all–rac–α–T, using acetic acid or acetic anhydride as acyl donors and a metal catalyst [23]. Previous research has documented the *in vivo* potency of α–TA in suppressing the metastasis of lung cancer cells [24] and triggering apoptosis in breast cancer cells (MCF–7) [25]. The conceptual framework for modifying the structure of α–T through its synthesis with fatty acids (e. g., pentanoic acid (PA), heptanoic acid (HA), and octanoic acid (OA)) aims to obtain potent derivatives of α–T. The synthesized compounds, specifically α-tocopherol pentanoate (α–TP), α–tocopherol heptanoate (α–TH), and α–tocopherol octanoate (α–TO), are expected to demonstrate antioxidant and anticancer activities. According to the (3-(4,5-dimethylthiazol-2-yl)-2,5-diphenyltetrazolium bromide (MTT) assay, the IC_{50} values for PA on MDA–MB–231/IR breast cancer cells were 7.87±1.2 mmol after 48 h of incubation [26] and 4.88±5.4 mmol after 72 h of incubation [27]. Meanwhile, the IC_{50} values for heptanoic acid (HA) on HepG2 liver cancer cells were 1.73±6.8 mmol after 48 h of incubation [28] and 0.89±6.4 mmol after 72 h of incubation [29]. OA enhanced the activity of caspase 8 [30] and cyclin-dependent kinase inhibitor 1 (P21) in all three cell types (colorectal cancer, skin cancer, breast cancer) [31]. Studies on the synthesis and activity of α–TP, α–TH, and α–TO are lacking. Hence, we synthesized α–TP, α–TH, and α–TO through the Steglich esterification method [32], and explored the possibility of their inhibitory effects on CII *in silico.*

MATERIALS AND METHODS

Materials

Organic solvents and chemicals were analytical grade and were purchased from Sigma Aldrich Co. (Indofa, Surabaya, Indonesia): *n*-hexane, chloroform, ethyl acetate, methanol, dimethyl sulfoxide

(DMSO), *N,N'*–dicyclohexylcarbodiimide (DCC), 4–dimethyl aminopyridine (DMAP), α–tocopherol (α–T), pentanoic acid (PA), heptanoic acid (HA), octanoic acid (OA), hydrochloric acid, triethylamine, anhydrous magnesium sulfate, and molecular sieve.

Aluminum sheets precoated with silica gel GF_{254} (Merck, Darmstadt, Germany) were used for thin-layer chromatography (TLC) and UV-scanned in the range of 200–400 nm. Column chromatography was carried out using silica gel G60 (70–230 mesh, Merck, Darmstadt, Germany). The UV spectra of α–TP, α–TH, and α–TO were recorded using a Hitachi UH5300 UV double-beam (visible/NIR) spectrophotometer. Fourier transform infrared (FTIR) spectra were recorded using a Shimadzu IR Prestige 21 FTIR spectrophotometer (Kyoto, Japan). Mass spectra (MS) were obtained from a Waters Xevo G2–XS QToF mass spectrometer (Milford, MA, USA).

Methods

Synthesis of the compounds (α-TP, α-TH, α-TO)

The esterification procedure followed the Steglich method [18], with DCC and DMAP as catalysts. PA (500 mg, 4.8957 mmol) was fully dissolved in chloroform (10 ml). Then, DCC (1.01 gram, 4.8957 mmol) and DMAP (59.8 mg, 0.4896 mmol) were added, and triethylamine (1 ml) was added dropwise. The synthetic reaction was conducted using a reflux apparatus at 50 °C for approximately 1–2 h. The reaction was continued by adding α–T (2.11 g, 4.8957 mmol) and stirring with a magnetic stirrer at 400 rpm for 24 h.

The white solid by–product (dicyclohexyl urea, DCU) was separated by filtration. The solvent in the filtrate was then evaporated, and the mixture was added to water (30 ml) and neutralized with HCl to a pH between 6 and 7. The reaction product was then transferred to a separating funnel and *n*-hexane (30 ml) was added. The uppermost layer (*n*–hexane layer) was then collected. Extraction was performed three times, and the obtained *n*–hexane layer was washed with water three times. Subsequently, anhydrous magnesium sulfate was added and the *n*–hexane layer was filtered to obtain an anhydrous extract. The extract was evaporated using a rotary evaporator until dry and the residue was purified through silica gel G60 column chromatography, eluted with 100% *n*–hexane. This resulted in the isolation of 1.5272 g of α–TP with a yield of 60.66%. The obtained product appeared as a yellowish oil with Rf = 0.63 in 9% ethyl acetate in *n*–hexane.

α–TH was prepared using the same procedure [18] as the synthesis of α–TP described above. HA (500 mg, 3.8408 mmol), chloroform (10 ml), DCC (792.4723 mg, 3.8408 mmol), DMAP (46.9255 mg; 0.3841 mmol), α–T (1.6543 g, 3.8408 mmol), and triethylamine (1 ml) were used. The pure α–TH showed a light–yellow color (1.2281 g, 58.90%, Rf = 0.70 in 9% ethyl acetate in *n*–hexane). Using the same procedure as with α–TP, OA (500 mg, 3.4671 mmol), chloroform (10 ml), DCC (715 mg, 3.4671 mmol), DMAP (45 mg, 0.3467 mmol), α–T (1.5 g, 3.4671 mmol), and triethylamine (1 ml) were employed to prepare α–TO. The pure α–TO appeared as a pale–yellow oil (1.1232 g, 58.20%, Rf = 0.65 in 9% ethyl acetate in *n*–hexane).

Structural analysis of the compounds (α–TP, α–TH, α–TO)

The structures of the compounds were elucidated using a UV–Vis spectrophotometer to identify the type of chromophore and the conjugated double bond based on the compound's maximum wavelength. The functional groups in all compounds were identified using FTIR in the range of 500–4000 cm^{-1}. LC–MS was utilized to determine the chromatographic patterns and fragmentation, identify the molecular mass of the absorption peaks, and validate the compound's purity.

Molecular docking study

The structure of the SDH in *Escherichia coli* (SQR) is closely analogous to CII [33]. The redox center of SQR plays a role in preventing the production of ROS on the flavin adenine dinucleotide (FAD) [34]. Hence, SQR is expressed during aerobic respiration to neutralize the activity of the fumarate reductase enzyme, known for its high production of ROS [34]. The SDH structure was acquired from the Protein Data Bank (PDB, http://www.rcsb.org) with the code 1NEK and had a resolution of 2.60 Å.

A Hewlett-Packard notebook (2018) featuring an Intel(R) Core™ i5-8250U CPU @1.60GHz, 8 GB RAM, and a Radeon 530 graphics card, and preloaded with the Windows 11 22H2 operating system was used to process the data. ChemDraw 18.1 and Chem3D 18.1 (PerkinElmer Informatics), AutoDock4.2 Tools Version 1.5.7, and BIOVIA Discovery Studio visualizer 21.1.0.0 (Discovery Studio 2021 Client, Dassault Systèmes) were used.

Ligand and protein preparation for *in silico* molecular docking

The macromolecular complex (1NEK) was separated from water solvent molecules and natural ligands. The macromolecule was optimized using AutoDock4.2 Tools Version 1.5.7, including the addition of polar hydrogens and Kollman charges. Finally, the file was saved in pdbqt format (.pdbqt) [35]. The natural ligand (FAD, $C_{27}H_{33}N_9O_{15}P_2$), used as a reference, was obtained from the PDB (http://www.rscb.org). Meanwhile, the test ligands (α-TP, α-TH, α-TO) were drawn, saved in cdx format (.cdx), and converted to pdb format using Chem3D 18.1 [36]. Both ligands were subjected to optimization with AutoDock4.2 Tools Version 1.5.7, incorporating a setting for adding hydrogen, charges, and a torsion tree. Afterward, the files were saved in pdbqt format (Protein Data Bank, partial charge (q), and atom type (t)) [37].

Redocking simulation with AutoDock4.2 tools

A grid box defines the spatial constraints for ligand docking on the macromolecule [38], set at coordinates (x = 80.925 Å; y = 88.698 Å; z = 146.511 Å) with a box volume of 60 Å x 42 Å x 40 Å. This was then saved in gpf format (grid parameter file). The next step involves selecting parameters using the Lamarckian GA method, to be applied in running AutoDock4.2 Tools Version, 1.5.7-which were saved in dpf format (docking parameter file).

The parameters resulting from the molecular docking were analyzed using AutoDock4.2 Tools. The docking parameters, including binding free energy (ΔG) values, inhibition constants (Ki), and root mean square deviation (RMSD), can be observed in the dlg file (docking log file) using the Notepad application. The interactions between ligands and the amino acid residues of enzyme were visualized using BIOVIA Discovery Studio visualizer 21.1.0.0 [38].

RESULTS

Synthesis of the compounds (α–TP, α–TH, α–TO)

Vitamin E derivatives were synthesized, and their anticancer activity was evaluated through molecular docking. In this study, the Steglich method [18], which involves esterification with DCC and DMAP catalysts, was used to synthesize three vitamin E derivatives. Steglich esterification typically occurs at room temperature, but in this case, the reaction was carried out at 50 °C. Elevating the temperature increases the reaction rate. Fig. 1 illustrates the reaction steps for the synthesis of the compounds.

The α–TP product was obtained in a yield of 60.66%, resulting in 1.5272 g of yellowish oil with an Rf value of 0.63 in 9% ethyl acetate in *n*–hexane. The pure α–TH exhibited a light–yellow color, with a yield of 58.90% (1.2281 g) and an Rf value of 0.70 in 9% ethyl acetate in *n*–hexane. The pale–yellow oil of pure α–TO was 1.1232 g (58.20%, Rf = 0.65 in 9% ethyl acetate in *n*–hexane). The pure α–TO (a pale–yellow oil) weighed 1.1232 g (58.20%, Rf = 0.65 in 9% ethyl acetate in *n*–hexane).

Structural analysis of the compounds (α–TP, α–TH, α–TO)

The UV spectral data showing the chromophore group and the maximum absorbance of compounds are presented in table 1. All compounds exhibited the maximum UV absorption at a wavelength of 204 nm, indicating the $n \rightarrow \pi^*$ electronic transition of the carbonyl (C=O) chromophore group in the ester. Thus, the three synthesized compounds belong to the ester type.

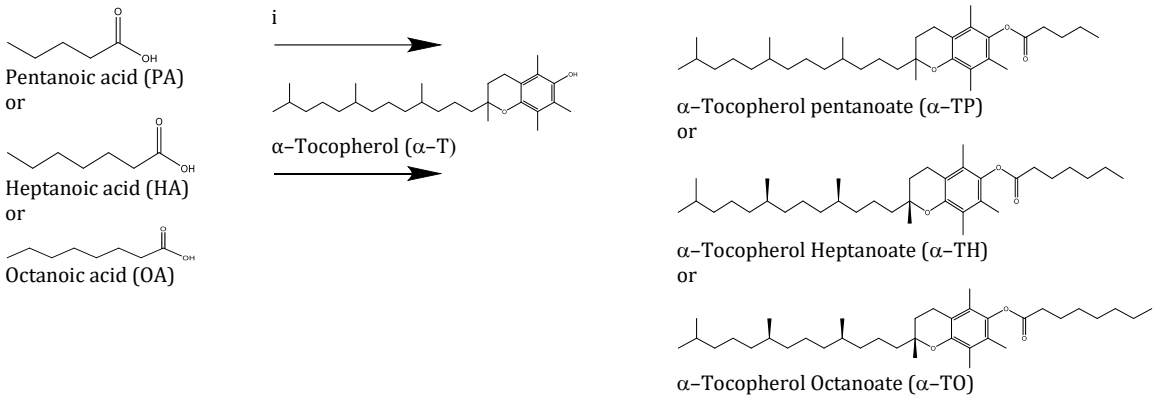

Fig. 1: The formation of an α-tocopherol pentanoate (α–TP), α–tocopherol heptanoate (α–TH), and α–tocopherol octanoate (α–TO). Reagents and conditions: i) chloroform, *N,N'*-dicyclohexylcarbodiimide (DCC), 4-dimethylaminopyridine (DMAP), triethylamine, 50 °C, 1–2 h reflux, ii) 50 °C, 24 h reflux

Table 1: Chromophore group and maximum absorbance produced by the compounds

Compound	Conc. (µg/ml)	λ max (nm)	Absorbance	Chromophore group	Compound type	Electronic transition
α–TP	1	204	0.146	C=O	Ester	n → π*
	5	204	0.470	C=O	Ester	n → π*
	10	204	0.838	C=O	Ester	n → π*
α–TH	1	203	0.182	C=O	Ester	n → π*
	5	204	0.293	C=O	Ester	n → π*
	10	204	0.772	C=O	Ester	n → π*
α–TP	1	204	0.145	C=O	Ester	n → π*
	5	204	0.340	C=O	Ester	n → π*
	10	203	0.639	C=O	Ester	n → π*

The results of the IR spectrum analysis indicate that all the generated compounds are esters with aliphatic CH groups (wavenumber of 2864–2924 cm^{-1}), carbonyl (C=O) groups in esters (wavenumber of 1754–1755 cm^{-1}), aliphatic $-CH_2-$ groups (wavenumber of 1458 cm^{-1}), aliphatic $-CH_3$ groups (wavenumber of 1374 cm^{-1}), C–O groups in esters (wavenumber of 1211–1246 cm^{-1}), and C–O groups in ethers (wavenumber of 1097–1147 cm^{-1}).

The LC-MS spectrum indicated peak ions for α–TP (M+H), α–TH ($M+NH_4$), and α–TO (M+H) at 515.26, 559.49, and 557.67 g/mol, respectively. This suggests that the actual molecular weights of α–TP, α–TH, and α–TO are 514.26, 542,889, and 556.67 g/mol, respectively. These molecular weights align with the calculations made using ChemDraw 18.1.

Redocking simulation and molecular docking with AutoDock4.2 tools

The RMSD values indicate the difference in the positions of ligand atoms compared to their natural state before the docking process [39]. A smaller RMSD value indicates minimal alteration to the natural state of the ligand. An acceptable RMSD deviation is typically less than 2.5 Å. The validation results of the natural ligands against the protein resulted in an RMSD of 2.11 Å, indicating the use of valid docking parameters. Hence, the docking method can be employed for the test ligands.

The results of molecular docking between the compounds with 1NEK are presented in table 2 and fig. 2. Molecular docking provides information on binding free energy (ΔG), inhibition constants (Ki), and the interaction between compounds and the protein.

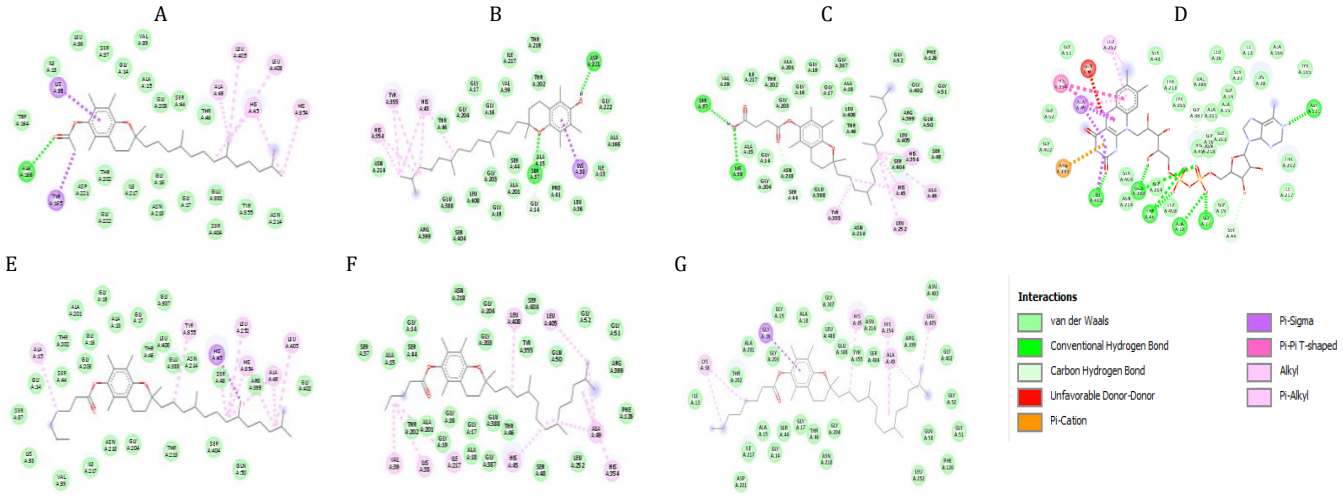

Fig. 2: Visualizing the docking results of 1NEK with α–TA (A), α–T (B), α–TS (C), FAD (D), α–TH (E), α–TP (F), and α–TO (G)

Table 2: Interaction between the amino acid residues of 1NEK and the compounds

Compound	ΔG (Kcal/mol)	Ki (μM)	Conventional hydrogen bond	Carbon hydrogen bond	Van der waals	Hydrophobic Bonds (Alkyl and pi-alkyl)	Pi-Sigma	Another bond
α–TA	-11.21	0.006	1 Ala166	0	Ala15 Asn214 Asn218 Asp221 Gly14 Gly16 Gly17 Gly203 Gly222 Ile36 Ile217 Leu36 Ser37 Ser44 Ser404 Thr46 Thr202 Trp164 Tyr355 Val39	5 Ala49 His45 His354 Leu405 Leu408	2 Lys38 Tyr165	0
α–T	-10.87	0.011	2 Asp221 Ser37	1 Gly14	Ala15 Ala166 Ala201 Arg399 Asn214 Glu388 Gly16 Gly17 Gly19 Gly203 Gly204 Gly222 Ile13 Ile217 Leu36 Leu408 Pro41 Ser44 Ser404 Thr46 Thr202 Thr219 Val39	3 His45 His354 Tyr355	1 Lys38	0
α–TS	-10.80	0.120	2 Ser37 Lys38	1 Ser44	Ala15 Ala18 Ala201 Arg399 Asn214 Asn218 Gln50 Glu388 Gly14 Gly16 Gly17 Gly18 Gly51 Gly52 Gly204 Gly387 Gly402 Ile217 Leu405 Leu408 Ser48 Phe126 Ser404 Thr46 Thr202 Val39	4 Ala49 His45 Leu252 Tyr355	1 His354	0
α–TH	-10.57	0.018	0	0	Ala18 Ala201 Arg399 Asn214 Asn218 Gln50 Glu388 Gly14 Gly16 Gly17 Gly19 Gly203 Gly204 Gly387 Gly402 His45 Ile217 Leu408 Lys38 Ser37 Ser44 Ser404 Thr46 Thr202 Thr213 Val39	6 Ala15 Ala49 His354 Leu252 Leu405 Tyr355	1 His45	0
α–TP	-9.61	0.090	0	0	Ala15 Ala18 Ala201 Arg399 Asn218 Gln50 Glu388 Gly14 Gly16 Gly17 Gly19 Gly51 Gly52 Gly203 Gly204 Gly387 Leu252 Phe126 Ser37 Ser44 Ser48 Ser404 Thr46 Thr202 Tyr355	8 Ala49 His45 His354 Ile217 Leu405 Leu408 Lys38 Val39	0	0
α–TO	-9.20	0.179	0	0	Ala15 Ala18 Ala201 Arg399 Asn214 Asn218 Asp221 Asn403 Gln50 Glu388 Gly14 Gly17 Gly19 Gly51 Gly52 Gly203 Gly204 Gly387 Gly402 Ile13 Ile217 Leu252 Leu408 Phe126 Ser44 Ser404 Thr46 Thr202 Tyr355	5 Ala49 His45 His354 Leu405 Lys38	1 Gly16	0
HA	-4.70	357.36	3 Arg399 Leu405 Ser404	0	Arg286 Asn403 Gln50 Glu255 Gly51 Gly52 Gly401 Gly402 Leu252 Thr254	3 Ala49 His242 Phe126	0	0
OA	-4.51	493.61	3 Gly402 Leu405 Ser404	0	Arg399 Asn214 Asn403 Glu388 Gly401 Phe126 Tyr355	3 Ala49 His45 His354	0	0
PA	-4.25	769.19	2 Arg399 Gly402	0	Asn403 Gln50 Gly51 Gly52 Gly401 His242 His354 Leu252 Phe126	2 Ala49 Leu405	0	0
AA	-3.48	2,820	2 Arg399 Gly402	0	Asn403 Arg286 Glu255 Gly401 His242 His354 Leu252 Phe126	0	0	0
Flavin-Adenine Dinucleotide (FAD)	-3.34	3,570	5 Ala18 Asp221 Glu388 Gly17 Leu405 Thr46	2 Gly19 Gly387	Ala15 Ala166 Ala201 Asn214 Asn218 Gly14 Gly16 Gly19 Gly51 Gly52 Gly203 Gly204 Gly402 His45 Ile13 Ile217 Leu36 Leu408 Lys38 Ser37 Ser48 Ser404 Thr202 Thr213 Tyr165 Tyr355 Val386	1 Leu255	1 Ala49	3 His354 Gln50 Arg399

DISCUSSION

The novel compounds in this study were synthesized through the combination of α–T and fatty acids (PA, HA, and OA). The–OH alcohol group in α–T acts as a feeble nucleophile, leading to a slow reaction rate when attacking the less reactive carbonyl carbon in fatty acids. Thus, a catalyst is necessary for the esterification reaction between α–T and fatty acids. Here, DCC and DMAP were used as catalyst in the Steglich esterification [32]. While this reaction typically takes place at room temperature, higher temperatures are employed in this study to accelerate the reaction. Chloroform serves as the inert solvent, and vitamin E exhibits high solubility in chloroform.

The nitrogen atom of DCC has free electron pairs that act as nucleophiles, attracting the hydrogen atom from fatty acids to form isourea (–N=C=N–) [40].

The nucleophilic nature of fatty acids arises from the removal of hydrogen atoms, leading to the presence of negatively charged oxygen. Isourea possesses a carbon center deficient in electrons, rendering it highly prone to assault by negatively charged nucleophiles, resulting in the formation of a reactive acyl intermediate known as *O*–acylisourea. DMAP serves as an acyl transfer agent, initiating an attack on *O*-acylisourea to generate a reactive amide intermediate (an active ester) [41]. This intermediate subsequently undergoes a swift reaction with α–T, resulting in the formation of α–tocopherol carboxylate with an ester bond.

The ongoing challenge in cancer treatment is primarily attributed to persistent mutations, rendering tumor cells resistant to conventional chemotherapeutic agents [42]. A contributing factor to the elevated incidence of cancer, its metastatic capability, and frequent resistance to treatment is the existence of tumor-initiating cells (TICs) [43]. These cells make up a small subset of the tumor, possessing the ability to self-renew and facilitate tumor growth [44]. Recent studies have shown the crucial role of TICs in the initiation and progression of tumors [45]. Consequently, targeted therapies aimed at TICs could impede tumor (re-) growth and potentially eliminate the pathology [46]. The exploration of anti-TIC approaches has thus becomes a research topic of interest. Mitocans, a class of compounds that have demonstrated anticancer properties through the destabilization of mitochondria, seems to to exhibit efficacy against TICs [21]. Mitocans are small compounds that induce apoptosis in cancer cells by targeting mitochondria [21]; they are categorized into various groups based on their molecular target. α-TS is an example of mitocan [47], which affects CII by disrupting the function of UbQ, leading to electron leakage and the production of ROS, in turn initiating selective apoptosis in cancer cells [47].

Our results showed a relationship between anticancer properties and the modification α–T by introducing an additional carboxylic substituent (e. g., pentanoate or, heptanoate or octanoate) at the C-6 position. The C–H groups of the novel compounds were tightly bonded to the active site of SDH by several van der Waals, hydrophobic, and electrostatic interactions. The absence of conventional hydrogen bonds seemed to have a minor impact on the affinity of the novel compounds with the SDH-like protein (fig. 2). Molecular docking of CII revealed that the free binding energies were in the ascending order of α–TO<α–TP<α–TH<α–TS<α–T<α–TA, with respective values of-9.20,-9.61,-10.57,-10.80,-10.87, and-11.21 kcal/mol.

Nonetheless, further studies *in vitro* and *in vivo* targeting CII are required to elucidate the anticancer activity of the synthesized compounds and validate their suitability as potential drug candidates. The outcomes of enzymatic and cytotoxic assays may differ from the *in silico* docking results and could provide new insights into the mechanism of action of the novel compounds.

CONCLUSION

The vitamin E derivatives α-tocopherol pentanoate (α-TP), α–tocopherol heptanoate (α-TH), and α–tocopherol octanoate (α-TO) were synthesized using the Steglich esterification method. All the synthesized compounds exhibited low binding affinity, demonstrating their lack of efficacy as potential cancer drug candidates. However, further research is needed to validate the inhibitory effects of the novel compounds *in vitro* and *in vivo* on mitochondrial CII in the most common types of cancer worldwide.

FUNDING

This study was financially supported by grants from Universitas Indonesia (PUTI Grant Number: ND-2994/UN2. F. D1.4/PPM.00.00/2023), Universitas Negeri Jakarta (Grant Number: 930/UN39//HK.02/2023), and RISET DAN INOVASI UNTUK INDONESIA MAJU (RIIM) (Contract Number: 22/IV/KS/05/2023 and 3823/UN30.15/PP/2023).

AUTHORS CONTRIBUTIONS

Irma Ratna Kartika: Conceptualization, Investigation, Methodology, Writing-original draft. Teni Ernawati: Conceptualization, Investigation, Methodology. Sri Widia A. Jusman: Conceptualization, Investigation, Methodology. Mohamad Sadikin: Conceptualization, Investigation, Methodology.

CONFLICT OF INTERESTS

All authors have no conflicts of interest

REFERENCES

1. Bandara AB, Drake JC, Brown DA. Complex II subunit SDHD is critical for cell growth and metabolism, which can be partially restored with a synthetic ubiquinone analog. BMC Mol Cell Biol. 2021;22(1):35. doi: 10.1186/s12860-021-00370-w, PMID 34118887.
2. Sun F, Huo X, Zhai Y, Wang A, Xu J, Su D. Crystal structure of mitochondrial respiratory membrane protein complex II. Cell. 2005;121(7):1043-57. doi: 10.1016/j.cell.2005.05.025, PMID 15989954.
3. Miyadera H, Shiomi K, Ui H, Yamaguchi Y, Masuma R, Tomoda H. Atpenins, potent and specific inhibitors of mitochondrial complex II (succinate-ubiquinone oxidoreductase). Proc Natl Acad Sci USA. 2003;100(2):473-7. doi: 10.1073/pnas.0237315100, PMID 12515859.
4. Russell CT, Kivelson MG. Detection of SO in Io's exosphere. Science. 2000;287(5460):1998-9. doi: 10.1126/science.287.5460.1998.
5. Jusman SWA, Azzizah IN, Sadikin M, Hardiany NS. Is the mitochondrial function of keloid fibroblasts affected by cytoglobin? Malays J Med Sci. 2021;28(2):39-47. doi: 10.21315/mjms2021.28.2.4, PMID 33958959.
6. Selak MA, Armour SM, MacKenzie ED, Boulahbel H, Watson DG, Mansfield KD. Succinate links TCA cycle dysfunction to oncogenesis by inhibiting HIF-α prolyl hydroxylase. Cancer Cell. 2005;7(1):77-85. doi: 10.1016/j.ccr.2004.11.022. PMID 15652751.
7. Aldera AP, Govender D. Gene of the month: SDH. J Clin Pathol. 2018;71(2):95-7. doi: 10.1136/jclinpath-2017-204677, PMID 29070651.
8. Owens KM, Aykin Burns N, Dayal D, Coleman MC, Domann FE, Spitz DR. Genomic instability induced by mutant succinate dehydrogenase subunit D (SDHD) is mediated by O_2−• and H_2O_2. Free Radic Biol Med. 2012;52(1):160-6. doi: 10.1016/j.freeradbiomed.2011.10.435, PMID 22041456.
9. Wang YM, Gu ML, Ji F. Succinate dehydrogenase-deficient gastrointestinal stromal tumors. World J Gastroenterol. 2015;21(8):2303-14. doi: 10.3748/wjg.v21.i8.2303, PMID 25741136.
10. Cairns P. Renal cell carcinoma. Cancer Biomark. 2010;9(1-6):461-73. doi: 10.3233/CBM-2011-0176, PMID 22112490.
11. Pinzariu O, Georgescu B, Georgescu CE. Metabolomics-a promising approach to pituitary adenomas. Front Endocrinol. 2018;9:814. doi: 10.3389/fendo.2018.00814, PMID 30705668.
12. Akirov A, Larouche V, Alshehri S, Asa SL, Ezzat S. Treatment options for pancreatic neuroendocrine tumors. Cancers. 2019;11(6):1-13. doi: 10.3390/cancers11060828, PMID 31207914.
13. Ugboko HU, Nwinyi OC, Oranusi SU, Fatoki TH, Omonhinmin CA. Antimicrobial importance of medicinal plants in Nigeria. Scientific World Journal. 2020;2020:7059323. doi: 10.1155/2020/7059323, PMID 33029108.
14. Lauritano C, Andersen JH, Hansen E, Albrigtsen M, Escalera L, Esposito F. Bioactivity screening of microalgae for antioxidant, anti-inflammatory, anticancer, anti-diabetes, and antibacterial activities. Front Mar Sci. 2016;3(68):1-2. doi: 10.3389/fmars.2016.00068.
15. Shahidi F, De Camargo AC. Tocopherols and tocotrienols in common and emerging dietary sources: occurrence, applications, and health benefits. Int J Mol Sci. 2016;17(10):1-29. doi: 10.3390/ijms17101745, PMID 27775605.
16. Traber MG, Atkinson J. Vitamin E, antioxidant and nothing more. Free Radic Biol Med. 2007;43(1):4-15. doi: 10.1016/j.freeradbiomed.2007.03.024, PMID 17561088.
17. Baharuddin NSB, Nasir NSB, Kamal NNSBNM, Saifuddin SNB, Mohamad SB. Vitamin E: an antioxidant with anticancer properties? Malays J Med Heal Sci. 2019;15(9):183-93.
18. Mohd Zaffarin AS, Ng SF, Ng MH, Hassan H, Alias E. Pharmacology and pharmacokinetics of vitamin e: nano formulations to enhance bioavailability. Int J Nanomedicine. 2020;15:9961-74. doi: 10.2147/IJN.S276355, PMID 33324057.
19. Yin C, Zhang C, Gao M. Enzyme-catalyzed synthesis of vitamin E succinate using a chemically modified nobody-435. Chin J Chem Eng. 2011;19(1):135-9. doi: 10.1016/S1004-9541(09)60189-0.
20. Liang L, Qiu L. Vitamin E succinate with multiple functions: a versatile agent in nanomedicine-based cancer therapy and its delivery strategies. Int J Pharm. 2021;600:120457. doi: 10.1016/j.ijpharm.2021.120457, PMID 33676991.
21. Panda V, Khambat P, Patil S. Mitocans as novel agents for anticancer therapy: an overview. Int J Clin Med. 2011;02(4):515-29. doi: 10.4236/ijcm.2011.24086.
22. Shiau CW, Huang JW, Wang DS, Weng JR, Yang CC, Lin CH. α-tocopheryl succinate induces apoptosis in prostate cancer cells in part through inhibition of Bcl-xL/Bcl-2 function. J Biol Chem. 2006;281(17):11819-25. doi: 10.1074/jbc.M511015200, PMID 16520381.
23. States U (12) Patent Application Publication (10) Pub. No: US. 2004/0092606A1;1(09); 2002-5.
24. Smolarek AK, Suh N. Chemopreventive activity of vitamin E in breast cancer: a focus on γ and δ-tocopherol. Nutrients. 2011;3(11):962-86. doi: 10.3390/nu3110962, PMID 22254089.
25. Lee E, Choi MK, Lee YJ, Ku JL, Kim KH, Choi JS. Alpha-tocopheryl succinate, in contrast to alpha-tocopherol and alpha-tocopheryl acetate, inhibits prostaglandin E2 production in human lung epithelial cells. Carcinogenesis. 2006;27(11):2308-15. doi: 10.1093/carcin/bgl073, PMID 16714329.
26. Han R, Nusbaum O, Chen X, Zhu Y. Valeric acid suppresses liver cancer development by acting as a novel HDAC inhibitor. Mol Ther Oncolytics. 2020;19:8-18. doi: 10.1016/j.omto.2020.08.017, PMID 33024815.

27. Jayaraj RL, Beiram R, Azimullah S, Mf NM, Ojha SK, Adem A. Valeric acid protects dopaminergic neurons by suppressing oxidative stress, neuroinflammation and modulating autophagy pathways. Int J Mol Sci. 2020;21(20):1-18. doi: 10.3390/ijms21207670, PMID 33081327.
28. Huang L, Gao L, Chen C. Role of medium-chain fatty acids in healthy metabolism: a clinical perspective. Trends Endocrinol Metab. 2021;32(6):351-66. doi: 10.1016/j.tem.2021.03.002, PMID 33832826.
29. Kimura I, Inoue D, Maeda T, Hara T, Ichimura A, Miyauchi S. Short-chain fatty acids and ketones directly regulate sympathetic nervous system via G protein-coupled receptor 41 (GPR41). Proc Natl Acad Sci USA. 2011;108(19):8030-5. doi: 10.1073/pnas.1016088108, PMID 21518883.
30. Narayanan A, Baskaran SA, Amalaradjou MAR, Venkitanarayanan K. Anticarcinogenic properties of medium chain fatty acids on human colorectal, skin and breast cancer cells *in vitro*. Int J Mol Sci. 2015;16(3):5014-27. doi: 10.3390/ijms16035014, PMID 25749477.
31. Zhang X, Xue C, Xu Q, Zhang Y, Li H, Li F. Caprylic acid suppresses inflammation via TLR4/NF-κB signaling and improves atherosclerosis in ApoE-deficient mice. Nutr Metab (Lond). 2019;16(1):40. doi: 10.1186/s12986-019-0359-2, PMID 31182969.
32. Neises B, Steglich W. Simple method for the esterification of carboxylic acids. Angew Chem Int Ed Engl. 1978;17(7):522-4. doi: 10.1002/anie.197805221.
33. Gong H, Gao Y, Zhou X, Xiao Y, Wang W, Tang Y. Cryo-EM structure of trimeric mycobacterium smegmatis succinate dehydrogenase with a membrane-anchor SdhF. Nat Commun. 2020;11(1):4245. doi: 10.1038/s41467-020-18011-9, PMID 32843629.
34. Cecchini G, Schroder I, Gunsalus RP, Maklashina E. Succinate dehydrogenase and fumarate reductase from *Escherichia coli*. Biochim Biophys Acta. 2002;1553(1-2):140-57. doi: 10.1016/s0005-2728(01)00238-9, PMID 11803023.
35. Zuhri UM, Purwaningsih EH, Fadilah F, Yuliana ND. Network pharmacology integrated molecular dynamics reveals the bioactive compounds and potential targets of *Tinospora crispa* Linn. as insulin sensitizer. Plos One. 2022;17(6):e0251837. doi: 10.1371/journal.pone.0251837, PMID 35737707.
36. Ernawati T. *In silico* analysis of the inhibitory potential of *Zingiber officinale* roscoe compounds against SARS-CoV-2. In: Proceedings of the 1st international conference for health research–BRIN (ICHR 2022); 2023. p. 360-73. doi: 10.2991/978-94-6463-112-8_34.
37. Jain NK, Agrawal A, Kulkarni GT, Tailang M. Molecular docking study on phytoconstituents of traditional ayurvedic drug tulsi (ocimum sanctum linn.) against COVID-19 mpro enzyme: an in silico study. Int J Pharm Pharm Sci. 2022;14(4):44-50. doi: 10.22159/ijpps.2022v14i4.43181.
38. Astiani R, Sadikin M, Eff ARY, Firdayani SFD. *in silico* identification testing of triterpene saponines on *Centella asiatica* on inhibitor renin activity antihypertensive. v14s2.44737. Int J Appl Pharm. 2022;14 Special Issue 2:1-4. doi: 10.22159/ijap.2022.
39. Mathew C, Lal N, SL, TRA, Varkey J. Antioxidant, anticancer and molecular docking studiesof novel 5-benzylidene substituted rhodanine derivatives. Int J Pharm Pharm Sci. 2023;15(7):7-19. doi: 10.22159/ijpps.2023v15i7.47421.
40. Teni Ernawati TE, Abdul Mun'im AM, Muhamad Hanafi MH, Arry Yanuar AY. Synthesis of cinnamamide derivatives and their α-glucosidase inhibitory activities. Sains Malays. 2020;49(2):315-22. doi: 10.17576/jsm-2020-4902-09.
41. Widiyarti G, Sundowo A, Megawati M, Ernawati T. Synthesis, characterization, anticancer and *in silico* ADME properties of caproic acid derivatives against P388 cancer cell lines. Indonesian J Pharm Sci Technol. 2019;1(2):1-8. doi: 10.24198/ijpst.v1i2.20192.
42. Mansoori B, Mohammadi A, Davudian S, Shirjang S, Baradaran B. The different mechanisms of cancer drug resistance: a brief review. Adv Pharm Bull. 2017;7(3):339-48. doi: 10.15171/apb.2017.041, PMID 29071215.
43. Marisa L, de Reynies A, Duval A, Selves J, Gaub MP, Vescovo L. Gene expression classification of colon cancer into molecular subtypes: characterization, validation, and prognostic value. PLOS Med. 2013;10(5):e1001453. doi: 10.1371/journal.pmed.1001453, PMID 23700391.
44. Visvader JE, Lindeman GJ. Cancer stem cells in solid tumours: accumulating evidence and unresolved questions. Nat Rev Cancer. 2008;8(10):755-68. doi: 10.1038/nrc2499, PMID 18784658.
45. Guinney J, Dienstmann R, Wang X, De Reynies A, Schlicker A, Soneson C. The consensus molecular subtypes of colorectal cancer. Nat Med. 2015;21(11):1350-6. doi: 10.1038/nm.3967, PMID 26457759.
46. O'Brien CA, Pollett A, Gallinger S, Dick JE. A human colon cancer cell capable of initiating tumour growth in immunodeficient mice. Nature. 2007;445(7123):106-10, doi: 10.1038/nature05372, PMID 17122772.
47. Neuzil J, Dyason JC, Freeman R, Dong LF, Prochazka L, Wang XF. Mitocans as anti-cancer agents targeting mitochondria: lessons from studies with vitamin E analogues, inhibitors of complex II. J Bioenerg Biomembr. 2007;39(1):65-72. doi: 10.1007/s10863-006-9060-z, PMID 17294131.